Behaviour of B–N–Si under high pressure and high temperature

H. YOSHIHARA*, A. ONODERA, K. SUITO
Faculty of Engineering Science, Osaka University, Toyonaka, Osaka 560, Japan
H. NAKAE‡, Y. MATSUNAMI§
Research Development Corporation of Japan, Chiyoda, Tokyo 100, Japan
T. HIRAI
Institute for Materials Research, Tohoku University, Aoba, Miyagi 980, Japan

The phase relations of the B–N–Si system have been studied using a quenching method up to 10 GPa and 2000° C using a high-pressure apparatus of the octahedral anvil type. Pressure–temperature conditions for obtaining z-BN (diamond analogue of boron nitride) were delineated for turbostratic BN (t-BN), t-BN/amorphous Si_3N_4 and t-BN/β-Si_3N_4. These conditions shift toward higher regimes of temperature as amorphous Si_3N_4 or β-Si_3N_4 is incorporated into t-BN. Spontaneous sintering occurring *in situ* at high pressure yields z-BN-based composite compacts.

1. Introduction

There has been rapidly growing interest in the production of composite materials in the search for new characteristics, feasibility, functions, and hence for applications. Composites are processed, in general, by reinforcing fibres, dispersion of powders, vapour deposition, implantation of ions, etc. (e.g. [1]).

We have previously reported [2] a new application of the chemical vapour deposition (CVD)/high pressure (HP) technique to the processing of z-BN (the zincblende form of boron nitride)-based composite ceramics. In that study, composites consisting of z-BN and nitrides, β-Si_3N_4 for instance, were fabricated *in situ* under pressure from amorphous B–N–Si. Because z-BN and its composites are important materials for industrial applications (e.g. [3]), a thorough understanding of the phase behaviour of the B–N–Si system under pressure is of great interest.

This work aimed to elucidate the phase behaviour of the B–N–Si system over a wide range of pressure and temperature. The turbostratic BN (t-BN), which assumes randomly oriented hexagonal networks [4], was studied first, followed by t-BN/amorphous Si_3N_4 (a-Si_3N_4) and t-BN/β-Si_3N_4.

2. Experimental procedure

2.1. Starting samples

Four different samples were prepared for starting materials by chemical vapour deposition technique [5, 6]. A mixture of BCl_3–NH_3–H_2 was employed to prepare t-BN. To prepare t-BN/a-Si_3N_4 or t-BN/β-Si_3N_4, $SiCl_4$ was incorporated into the mixture. Vaporization was carried out under a pressure of 1.3 kPa. The samples were deposited on to a graphite substrate heated to 1400° C for t-BN and t-BN/a-Si_3N_4 or to 1800° C for t-BN/β-Si_3N_4. The Si_3N_4 contents, estimated from wet chemical analysis, were 3.52 or 10.6 wt % for a-Si_3N_4 and 10.6 wt % for β-Si_3N_4, respectively.

Fig. 1 shows infrared absorption spectra for t-BN/a-Si_3N_4 and t-BN/β-Si_3N_4. In the spectrum of

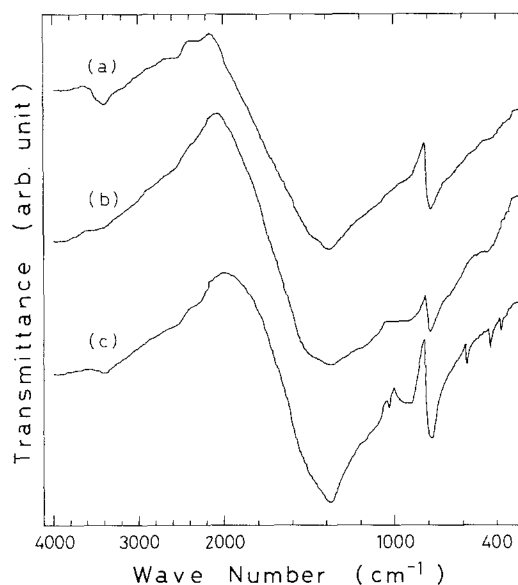

Figure 1 Infrared spectra of the starting samples. (a) t-BN/a-Si_3N_4 (3.52 wt %); (b) t-BN/a-Si_3N_4 (10.6 wt %); (c) t-BN/β-Si_3N_4 (10.6 wt %).

**Present address*: Chemical Todgosei Industry Co., Minato, Nagoya 455, Japan.
‡*Present address*: Furukawa Electric Co., Chiyoda, Tokyo 100, Japan.
§*Present address*: Japan Metals and Chemicals Co., Tsukuba, Ibaraki 305, Japan.

0022-2461/90 $03.00 + .12 © *1990 Chapman and Hall Ltd.*

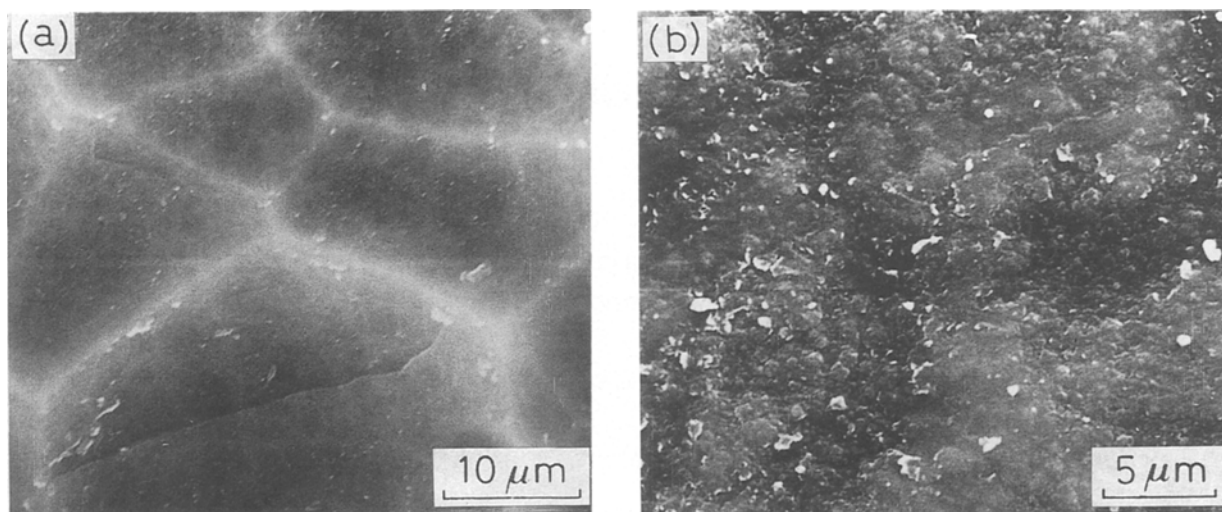

Figure 2 Scanning electron micrographs of the starting samples. (a) t-BN/a-Si_3N_4 (3.52 wt %); (b) t-BN/β-Si_3N_4 (10.6 wt %).

t-BN/a-Si_3N_4 (3.52 wt %) (Fig. 1a), strong absorption bands characteristic of t-BN [7] are observed at 1380 and 790 cm^{-1}. For t-BN/a-Si_3N_4 (10.6 wt %) (Fig. 1b), broad bands centred at 980 and 480 cm^{-1} become conspicuous, reflecting the increased amount of amorphous Si_3N_4 [8]. In the spectrum of t-BN/β-Si_3N_4 (10.6 wt %) (Fig. 1c), absorption bands for β-Si_3N_4 (at 1040, 910, 580, 445 and 380 cm^{-1}) [8] are observed, in addition to the absorptions arising from t-BN.

Fig. 2 shows scanning electron micrographs for t-BN/a-Si_3N_4 (3.52 wt %) and t-BN/β-Si_3N_4 (10.6 wt %). In t-BN/a-Si_3N_4 (3.52 wt %) (Fig. 2a), each grain contains smaller grains about 1 μm in size. In t-BN/β-Si_3N_4 (10.6 wt %) (Fig. 2b), grains ($\sim$ 10 μm) with a flaky structure are observed. Transmission electron microscopy observation of the sample has revealed that β-Si_3N_4 single crystals in sizes from 30 to 50 nm are dispersed within t-BN [9].

2.2. High-pressure treatment

Each sample prepared in Section 2.1 was pulverized and enclosed in an octahedral sample cell shown in Fig. 3. High pressure was generated in an octahedral anvil-type apparatus [10, 11]. The pressure was known from calibrations using fixed points [12, 13]. High temperature was attained by passing an alternating current through a graphite tube, which also served as a sample container. The temperature was measured using a Pt–Pt/Rh (13%) or W/Re (5%)–W/Re (26%) thermocouple. No correction was made for the effect of pressure on the e.m.f. of the thermocouples. The high temperature was held for 10 min in most cases.

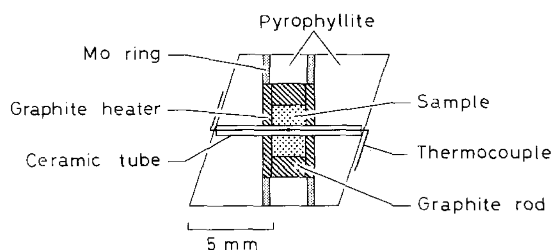

Figure 3 Cross-section of an octahedral sample cell for high-pressure experiments.

2.3. Post-compression measurements

After the sample was quenched to room temperature, the pressure was released. The sample was then recovered and subjected to X-ray diffraction (XRD) analysis, SEM observation, X-ray microanalysis (XMA), and infrared absorption measurements. For sintered compacts, Vickers microhardness, H_v, was measured under a load of 4.9 N. Young's modulus was also measured using a pulse-echo overlap ultrasonic method [14]. The fracture toughness, K_{Ic} [15], was obtained from microscopic observation of crack lengths at the indentation fractures.

3. Results

3.1. Phase relations

3.1.1. t-BN

Pressure–temperature conditions and phases obtained from t-BN are plotted in Fig. 4. The amounts of each phase were estimated from characteristic peaks in the powder X-ray diffraction patterns for the recovered samples. At 6 GPa, the phase obtained was solely the graphite-type BN (g-BN). At 7 GPa, z-BN appears at temperatures higher than 900° C. From Fig. 4 threshold conditions for obtaining z-BN are found to be 7 GPa and 900° C.

Fig. 5 shows X-ray diffraction patterns for the

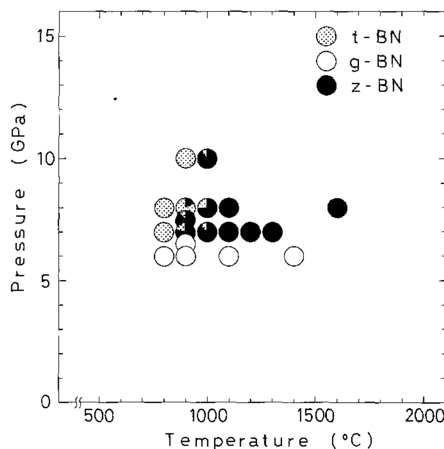

Figure 4 Pressure–temperature conditions and phases obtained from t-BN after 10 min duration.

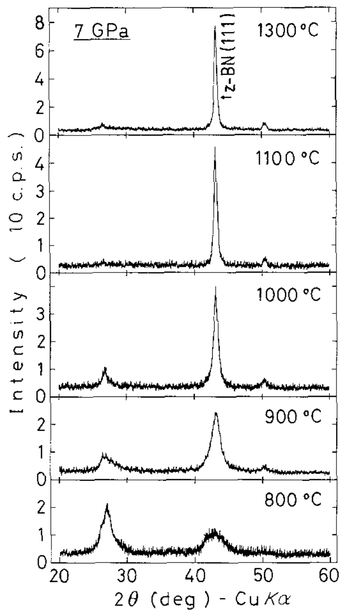

Figure 5 X-ray diffraction patterns of recovered samples started with t-BN and heat-treated at 7 GPa for 10 min.

samples prepared with t-BN and recovered after heat treatment at 7 GPa. The sample remains t-BN at 800° C. At 900° C the z-BN (1 1 1) reflection appears with a broad peak, suggesting that t-BN is directly converted into z-BN. This observation of direct conversion has been reported by Gladkaya *et al.* [16]. On increasing the temperature beyond 1000° C, the z-BN (1 1 1) reflection is strengthened further.

3.1.2. t-BN/a-Si_3N_4 (3.52 wt %)

Fig. 6 shows plots of pressure–temperature conditions and phases obtained from t-BN/a-Si_3N_4 (3.52 wt %). Obviously, g-BN appears over a range wider than in the case of t-BN (Fig. 4). The threshold conditions for obtaining z-BN are 6 GPa and 1600° C, or 7 GPa and 1400° C. A small amount of β-Si_3N_4 is observable at temperatures between 1500 and 1700° C at 7 GPa. The temperature needed for the occurrence of β-Si_3N_4 is reduced slightly when the pressure is raised to 8 or 10 GPa.

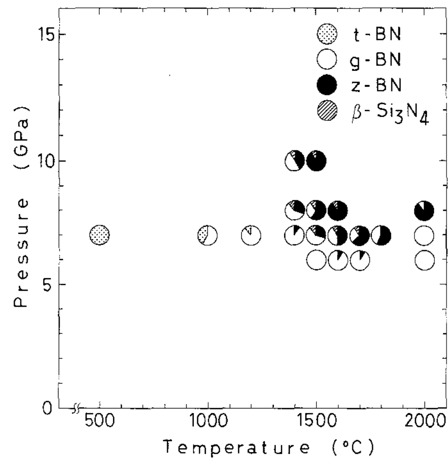

Figure 6 Pressure–temperature conditions and phases obtained from t-BN/a-Si_3N_4 (3.52 wt %) after 10 min duration.

Figs 7a and b show X-ray diffraction patterns for the samples prepared with t-BN/a-Si_3N_4 (3.52 wt %) and recovered after heat treatment at 7 GPa. In Fig. 7a the sample remaining t-BN below 500° C is converted into g-BN at 1000° C, and this g-BN grows at higher temperatures. z-BN also begins to appear at 1400° C. Two reflections from β-Si_3N_4 are observed at 1500° C.

In Fig. 7b, the coexistence of g-BN and z-BN together with increased prevalence of z-BN upon consumption of g-BN is observed up to 1800° C. As the equilibrium line between g-BN and t-BN is approached [17], z-BN formed below 1800° C is reconverted into g-BN and vanishes at 2000° C.

3.1.3. t-BN/a-Si_3N_4 (10.6 wt %)

Fig. 8 shows X-ray diffraction patterns of the samples prepared with t-BN/a-Si_3N_4 (10.6 wt %) and heated at 7 GPa. The samples remain amorphous below 1500° C. Both z-BN and β-Si_3N_4 appear at 1600° C and the

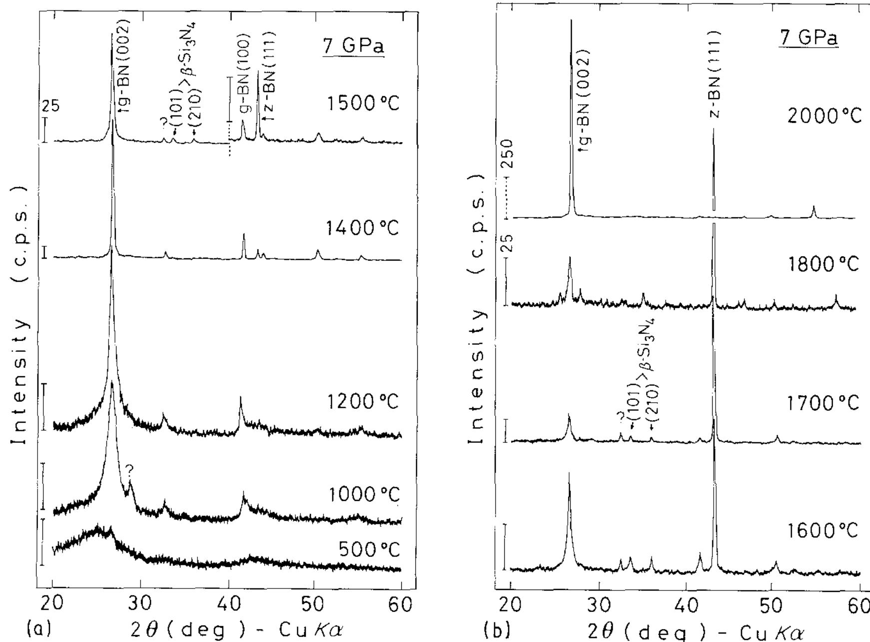

Figure 7 X-ray diffraction patterns of recovered samples prepared with t-BN/a-Si_3N_4 (3.52 wt %) and heat treated at 7 GPa for 10 min. (a) Below 1500° C, (b) above 1600° C.

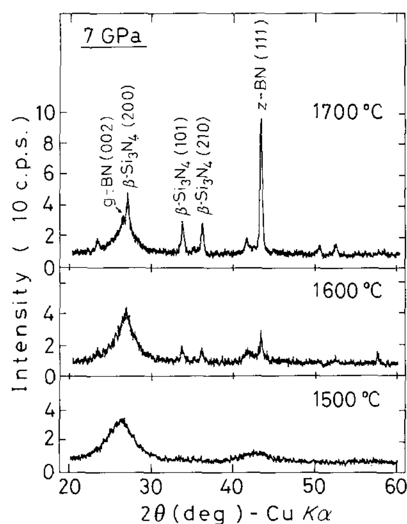

Figure 8 X-ray diffraction patterns of recovered samples prepared with t-BN/a-Si_3N_4 (10.6 wt %) and heat treated at 7 GPa for 10 min.

diffraction peaks of the two forms strengthen at 1700° C. Formation of g-BN is minor, suggesting that z-BN is formed to a greater part directly from t-BN. The threshold temperature for the occurrence of z-BN at 7 GPa becomes higher by approximately 200° C as the amount of a-Si_3N_4 is increased from 3.52 to 10.6 wt %.

3.1.4. *t-BN/β-Si_3N_4 (10.6 wt %)*

Pressure–temperature conditions and phases obtained from t-BN/β-Si_3N_4 (10.6 wt %) are plotted in Fig. 9. The threshold conditions for z-BN formation are 1300° C at 7 GPa, or 1400° C at 6 GPa. The amount of z-BN formed under these conditions is small. The inherent β-Si_3N_4, contained as 10.6 wt % in the starting sample, appears over the entire range studied. At pressures above 8 GPa, z-BN is obviously formed directly from t-BN, without the formation of g-BN.

Fig. 10 shows X-ray diffraction patterns of the samples prepared with t-BN/β-Si_3N_4 (10.6 wt %) and recovered after heat treatment at 7 GPa. The sample retains t-BN below 1200° C. At 1400° C, conversion of t-BN into g-BN takes place, concurrently with the appearance of z-BN. As the temperature is raised further, the amount of g-BN decreases whereas z-BN becomes prevalent.

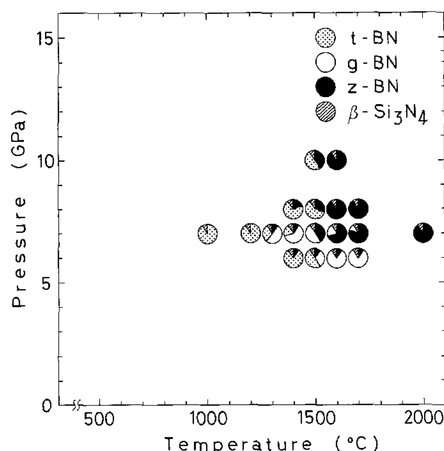

Figure 9 Pressure–temperature conditions and phases obtained from t-BN/β-Si_3N_4 (10.6 wt %) after 10 min duration.

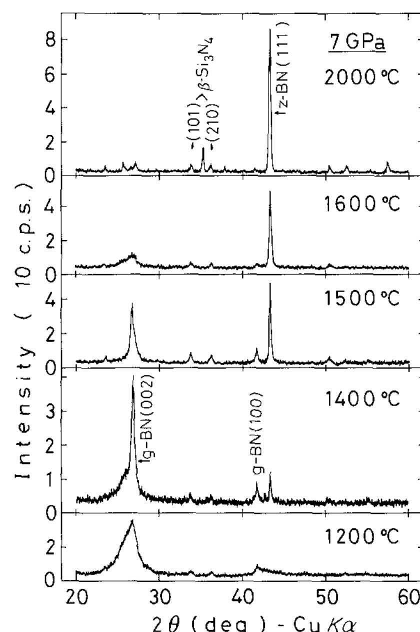

Figure 10 X-ray diffraction patterns of recovered samples prepared with t-BN/β-Si_3N_4 (10.6 wt %) and heat treated at 7 GPa for 10 min.

3.2. Reaction boundaries

Fig. 11 shows pressure–temperature boundaries for obtaining z-BN from various starting materials by amounts higher than 50%. Lines A, C and E are from previous reports; A from amorphous BN (a-BN) [18], C from incompletely crystallized g-BN [19] and E from well-crystallized g-BN [20]. Lines B, D and F are from this study; B from t-BN, D from t-BN/a-Si_3N_4 (3.52 wt %) and F from t-BN/β-Si_3N_4 (10.6 wt %). Also shown in Fig. 11 is the thermodynamically calculated equilibrium between g-BN and z-BN [17].

Examination of lines B, D and F in Fig. 11 clarifies that the incorporation of Si_3N_4 into t-BN, in the form of either a-Si_3N_4 or β-Si_3N_4, thrusts the reaction boundary towards a higher temperature regime. Lines D and F are located close to each other and also to line E, although the slope of line D is negative relative to the pressure coordinate. Thus, the conditions for z-BN formation become similar to those for well-crystallized g-BN [20].

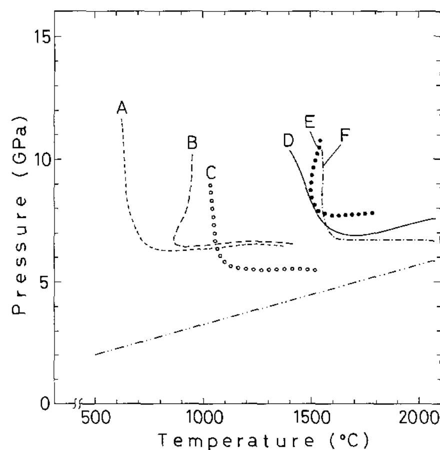

Figure 11 Pressure–temperature boundaries for forming z-BN from various starting samples: (A) From a-BN [18], (B) from t-BN, (C) from incompletely crystallized g-BN [19], (D) from t-BN/a-Si_3N_4 (3.52 wt %), (E) from well-crystallized g-BN [20], (F) from t-BN/β-Si_3N_4 (10.6 wt %). (—··—) Thermodynamically calculated equilibrium between g-BN and z-BN.

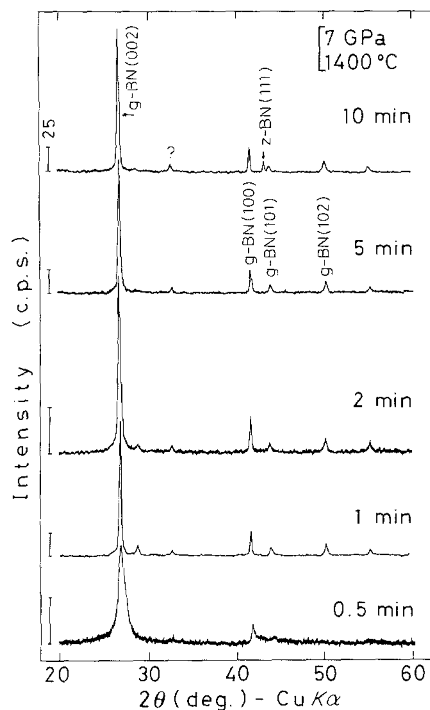

Figure 12 Time-resolved X-ray diffraction patterns for t-BN/a-Si_3N_4 (3.52 wt %) at 7 GPa and 1400° C.

3.3. Kinetics

Fig. 12 shows time-resolved X-ray diffraction patterns for t-BN/a-Si_3N_4 (3.52 wt %). The sample was held at 7 GPa and 1400° C. After each prolonged time, the sample was recovered and X-rayed. Within 1 min the sample undergoes formation of g-BN from t-BN. The g-BN (0 0 2) reflection is very strong and sharp. Also, two reflections, (1 0 1) and (1 0 2), from g-BN, each arising from three-dimensional order, appear at 43.9° and 50.2°. The prolongation of time virtually does not alter the g-BN diffraction pattern, indicating that the formation of g-BN is completed within 1 min. On the other hand, the z-BN (1 1 1) reflection appears at 43.1° only after 10 min, which shows that the formation of z-BN from t-BN/a-Si_3N_4 (3.52 wt %) proceeds rather slowly at 7 GPa and 1400° C.

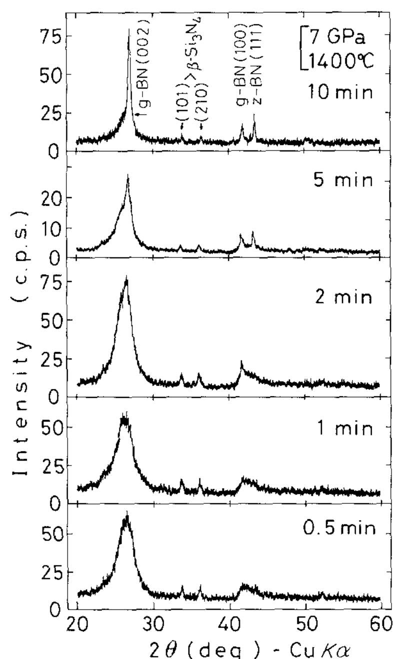

Figure 13 Time-resolved X-ray diffraction patterns for t-BN/β-Si_3N_4 (10.6 wt %) with 7 GPa and 1400° C.

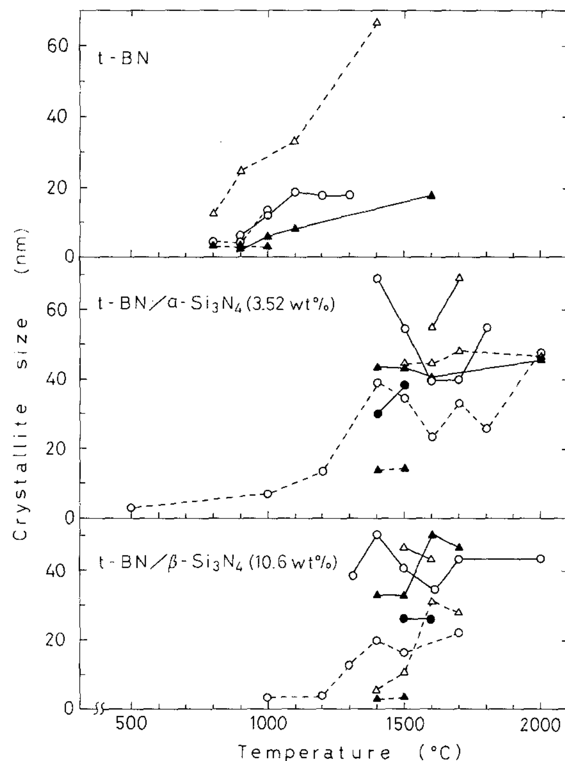

Figure 14 Change of the crystallite size of (– – –) t-BN and g-BN, and (——) z-BN obtained from three different starting samples at various pressures: (●) 10 GPa, (▲) 8 GPa, (○) 7 GPa, (△) 6 GPa.

Fig. 13 shows time-resolved X-ray diffraction patterns for t-BN/β-Si_3N_4 (10.6 wt %) also at 7 GPa and 1400° C. During the early stages, 0.5 and 1 min, essentially no change occurs in the diffraction patterns. After 2 min, the g-BN (0 0 2) peak appears. This g-BN peak becomes strengthened after 5 min, while the z-BN (1 1 1) peak also appears. No reflections from the g-BN (1 0 1) and (1 0 2) appear, suggesting that the g-BN formed remains incompletely crystallized.

3.4. Crystallite size

Fig. 14 shows the change of crystallite size of g-BN (or t-BN) and z-BN as a function of temperature at various pressures. The sizes of the crystals were estimated from the characteristic peaks in the X-ray diffraction patterns using Scherrer's equation (e.g. [21]).

The crystallite size of g-BN (or t-BN) remarkably increases with temperature at 6 GPa but remains unaltered at 7 and 8 GPa when t-BN is used as the starting material (dashed lines in the top section in Fig. 14). From t-BN/a-Si_3N_4 (3.52 wt %), the crystallite sizes of g-BN (t-BN) become saturated above 1400° C at pressures from 6 to 8 GPa (dashed lines in the middle section in Fig. 14). The growth of g-BN (t-BN) crystals from t-BN/β-Si_3N_4 (10.6 wt %) is slower; the sizes after saturation are smaller (dashed lines in the bottom section in Fig. 14).

At 7 and 8 GPa, z-BN crystals from t-BN begins to grow at about 900° C, but the size remains rather small (solid lines in the top section in Fig. 14). From t-BN/a-Si_3N_4 (3.52 wt %), z-BN crystals are already large in size even at the threshold temperature for their appearance and do not exhibit further growth at higher

temperatures (solid lines in the middle section in Fig. 14). This virtual saturation in crystal growth is more clearly demonstrated by the z-BN formation from t-BN/β-Si_3N_4 (10.6 wt %) (solid lines in the bottom section in Fig. 14).

It should be noted that the crystallite size exhibits maxima at 6 or 7 GPa for z-BN from t-BN/a-Si_3N_4 (3.52 wt %) and at 6 to 8 GPa for z-BN from t-BN/β-Si_3N_4 (10.6 wt %). It should also be noted that the z-BN crystallite size grown from both t-BN/a-Si_3N_4 (3.52 wt %) and t-BN/β-Si_3N_4 (10.6 wt %) is the smallest at 10 GPa, the highest pressure studied in this work. The occurrence of a maximum and the decrease in the crystallite size relative to pressure are in accord with our suggestions put forward in a previous paper [2].

3.5. Infrared spectra

Fig. 15 compares i.r. spectrum of the sample recovered from 8 GPa and 1700° C with that of the starting t-BN/β-Si_3N_4 (10.6 wt %). The strong bands centred at 1400 and 800 cm^{-1} in the spectrum of the starting material have vanished after the high pressure–high temperature treatment. Instead, a band centred at 1100 cm^{-1} appears in the high-pressure product. This band is ascribed to z-BN [22].

In Fig. 15, the bands arising from β-Si_3N_4 contained in the starting material are all observable in the high-pressure product, indicating again that the inherent β-Si_3N_4 remains unchanged in structure after the high pressure–high temperature treatment. A band grows at 460 cm^{-1}. This, together with the new band centred at 600 cm^{-1}, have not yet been identified.

3.6. Mechanical properties

Some of the recovered samples were obtained as well-sintered compacts. The sintering took place through the formation of z-BN; it also occurs spontaneously *in situ* under pressure. XMA on the sintered compacts revealed a homogeneous distribution of β-Si_3N_4 among z-BN crystals. The sintered compacts are thus z-BN-based composites containing β-Si_3N_4, whether inherent or those crystallized from the amorphous state.

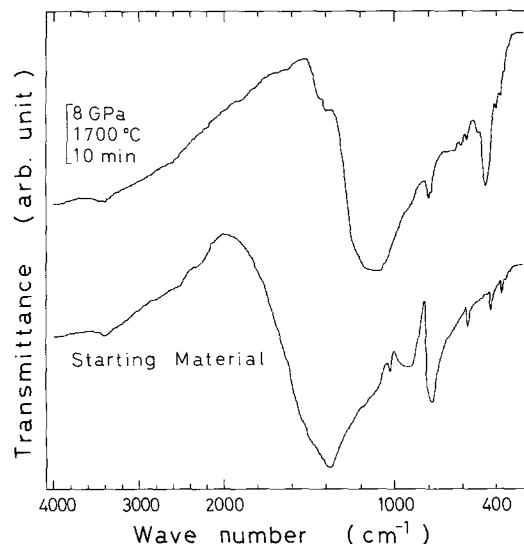

Figure 15 Infrared spectra for t-BN/β-Si_3N_4 (10.6 wt %).

Table I lists Vickers microhardness for such sintered compacts. Relevant hardness data for some other compacts [2, 23–29] are also listed. In this study the highest hardness is given by the compact from t-BN/β-Si_3N_4 (10.6 wt %) sintered at 10 GPa and 1600° C. All the compacts from t-BN/β-Si_3N_4 (10.6 wt %) constitute the upper bound for the microhardness of all BN-based composite compacts.

Table II gives Young's modulus and fracture toughness of the composite compact sintered at 8 GPa and 1600° C from t-BN/β-Si_3N_4 (10.6 wt %). Also shown in Table II for comparison are data from some typical ceramics [22, 30, 31]. The composite compact from this study gives a Young's modulus between those of z-BN and β-Si_3N_4 and a fracture toughness close to those of β-Si_3N_4, Al_2O_3 and SiC.

4. Discussion

4.1. Phase behaviour

Four different samples have been studied in this work. Each sample yields z-BN after high pressure–high temperature treatments. g-BN and β-Si_3N_4 are also formed, depending on the samples. The occurrence of these phases at 7 GPa from the four samples is sum-

TABLE I Microhardness for sintered compacts of z-BN and related ceramics

Starting sample	High-pressure treatment			Microhardness H_v or H_k (GPa)	Reference
	Pressure (GPa)	Temperature (° C)	Time (min)		
t-BN/β-Si_3N_4 (10.6 wt %)	10	1600	10	49 ~ 60	Present work
	8	1700	10	46 ~ 57	Present work
	8	1600	10	45 ~ 56	Present work
t-BN/a-Si_3N_4 (3.52 wt %)	8	2200	10	23 ~ 30	Present work
a-BN/a-Si_3N_4 (54.1 wt %)	7	2200	10	29 ~ 40	[2]
	7	1800	10	30 ~ 38	[2]
	6	2000	10	32 ~ 47	[2]
g-BN + AlN	5.5	1600	15	45	[23]
w-BN + a-Si_3N_4	6.3 ~ 6.5	1500 ~ 1700	15	30 ~ 40	[24]
z-BN + TiC/TiN + Al	5.8	1450	20	34	[25]
g-BN	6	1450	15	60 ~ 70	[26]
w-BN	6.7	1450 ~ 1600	15	65 ~ 76	[27, 28]

TABLE II Young's modulus, E, and fracture toughness, K_{IC} of some ceramics

Material	E (GPa)	K_{IC} (MPa m$^{1/2}$)	Reference
z-BN/β-Si_3N_4	570	> 5.5	Present work
z-BN	700	–	Calculated from elastic constants data in [22]
β-Si_3N_4	300	6	[30]
Al_2O_3	400	5	[30]
SiC	400	4	[30]
Partially stabilized ZrO_2	210	9	[31]

marized in Table III in terms of the threshold temperatures obtained from Figs 4, 6, 8 and 9.

In Table III, the major effects of incorporating Si_3N_4 in t-BN are seen to be two-fold. First, it induces g-BN formation which otherwise does not occur in pure t-BN at 7 GPa. An increase in the incorporated amount of a-Si_3N_4 gives rise to an increase in the threshold temperature for the g-BN formation. For 10.6 wt % Si_3N_4, incorporation of the β-form rather than the amorphous yields a lower threshold temperature. Second, the incorporation causes an upward shift of the threshold temperature for z-BN formation. The shift relative to the amounts and forms of Si_3N_4 exhibits a rough correspondence to the g-BN formation.

These two effects may be simply accounted for by an expansion of interplanar spacings in t-BN caused by the incorporation of Si_3N_4. The direct g-BN to z-BN conversion becomes retarded by this expansion and instead the metastable g-BN appears as an intermediate. The higher amount of Si_3N_4 results in a larger expansion and hence a stronger retardation. Incorporation of the crystalline form, β-Si_3N_4, however, minimizes the amount of expansion and consequently the retardation is prevented to some extent.

In Table III, the formation of β-Si_3N_4 from a-Si_3N_4 occurs approximately at the same temperatures for the z-BN formation. The formation of z-BN is, in this case, from g-BN (or t-BN) and hence is associated with a break of the hexagonal layered bonds followed by reconstruction into the tetrahedral configuration in the zincblende structure. Upon the crystallization of a-Si_3N_4, the non-molecular random network [8] turns into the planar configuration [8] in β-Si_3N_4. Although z-BN differs from β-Si_3N_4 in the configuration, the formation of the two phases is similar in that they are associated with a relatively large rearrangement of bonds and volume reduction as well. The two formations can then be cooperative with each other, and hence the z-BN formation may trigger the β-Si_3N_4 formation and vice versa, possibly leading to a concurrence of z-BN and β-Si_3N_4 at the same temperature.

TABLE III Threshold temperatures for the formation of g-BN, z-BN and β-Si_3N_4 at 7 GPa

Starting sample	Threshold temperature (° C)		
	g-BN	z-BN	β-Si_3N_4
t-BN	–	900	Not included
t-BN/a-Si_3N_4 (3.52 wt %)	1000	1400	1500
t-BN/a-Si_3N_4 (10.6 wt %)	1600	1600	1600
t-BN/β-Si_3N_4 (10.6 wt %)	1300	1300	Inherent

Because of the concurrent formation of z-BN and β-Si_3N_4, there might occur an exchange of bondings between the two species, producing new bonds, for instance B–Si. This is supported, in part, by the appearance of the unknown peak at an angle 32.7° in the X-ray diffraction pattern (Fig. 7) of the high-pressure products from t-BN/a-Si_3N_4 (3.52 wt %). This peak was also observed in most of the high-pressure products from t-BN/a-Si_3N_4 (10.6 wt %). The 32.7° peak, corresponding to an interplanar spacing of 0.275 nm, is the second strongest reflection of B_4Si [32]. The strongest reflection of B_4Si, from the spacing of 0.267 nm is, however, eventually disturbed by the β-Si_3N_4 (1 0 1) peak, and hence formation of B_4Si cannot be fully evinced.

The formation of g-BN is competitive with z-BN formation, as is known from the kinetic data. In Fig. 12, g-BN is formed quite rapidly and well crystallized, while the formation of z-BN is slow from t-BN/a-Si_3N_4 (3.52 wt %). By contrast, from t-BN/β-Si_3N_4 (10.6 wt %) (Fig. 13) z-BN formation is rather rapid and instead the g-BN formed is incompletely crystallized. These facts and the data from t-BN/a-Si_3N_4 (10.6 wt %) (Fig. 8) indicate that the higher amount in Si_3N_4, whether amorphous or crystalline, enhances z-BN formation when in competition with g-BN formation.

The crystallization of a-Si_3N_4 incorporated into t-BN occurs only in the β-form. No α-Si_3N_4 is observed over the entire range of pressure–temperature studied for the two samples with different a-Si_3N_4 contents. Because the densities of the two crystalline forms of Si_3N_4 are the same [33], any factor(s) other than the density must govern the dominant formation of β-Si_3N_4. In fact, Shimada *et al.* [34, 35] observed α-Si_3N_4 formation below about 1500° C at pressures between 1.5 and 6 GPa and attributed the predominance of the phases to an impurity effect [35]. However, Prochazka and Rocco reported a dominant formation of β-Si_3N_4 from various kinds of a-Si_3N_4 at 5 GPa and above 1500° C [29]. Thus, temperature is also a factor governing the dominance of the phases; lower temperature for α-form and higher temperature for β-form. Because the crystallization of a-Si_3N_4 is concurrent with the z-BN formation as mentioned earlier, no crystalline form of Si_3N_4 could appear below 1400° C, the lowest temperature for the concurrence of z-BN and β-Si_3N_4 (Table III). At temperatures higher than this, the crystallization of a-Si_3N_4 must occur in the β-form because of the higher temperature.

The wurtzitic form of BN (w-BN) is as dense as z-BN [36], yet no w-BN is formed in any of the samples studied here. The formation of w-BN has been reported to occur specifically from well-crystallized g-BN [20, 37, 38]. Also, the rhombohedral form of BN [39] and amorphous BN [18] can form w-BN. A conversion of w-BN into z-BN upon heating under pressure has been unanimously observed [20, 38–40]. The prevalence of z-BN over w-BN under high pressure–high temperature conditions is therefore similar to that of the β-form over the α-form in Si_3N_4.

4.2. Sintered composites

The composite compacts obtained from t-BN/β-Si_3N_4 (10.6 wt %) exhibit high values of microhardness (Table I) as well as of fracture toughness. The inherent β-Si_3N_4 precludes the volume reduction which otherwise is associated with the crystallization from the amorphous state. The volume reduction can sometimes cause cracks between the sintered grains and weakens the compacts sintered. The inherent β-Si_3N_4 is more favourable for enhancing the mechanical properties of the compacts.

The higher microhardness for the 10 GPa compact compared to the 8 GPa compacts from t-BN/β-Si_3N_4 (10.6 wt %) (Table I) can be accounted for by higher densification due to the higher pressure. In addition, the crystallite size of z-BN decreases with increasing pressure while there is essentially no change in the size with increase of temperature (Fig. 14). The higher microhardness of the 10 GPa compact can, therefore, also be ascribed to the smaller size of the z-BN crystallites composing the compact.

5. Conclusions

Incorporation of Si_3N_4 into t-BN pushes the temperatures needed for the occurrence of z-BN toward higher regimes by approximately 400° C or more at 7 GPa. The form of Si_3N_4 governs, to some extent, the formation of z-BN and correspondingly of g-BN. Upon heating t-BN at 7 GPa, z-BN is formed directly. Likewise, in the case of t-BN/a-Si_3N_4 (10.6 wt %), the z-BN formation is primarily by a direct path from t-BN. Formation of z-BN via g-BN proceeds in t-BN/a-Si_3N_4 (3.52 wt %) and in t-BN/β-Si_3N_4 (10.6 wt %).

The crystallite sizes of z-BN, in the order of 10 nm, exhibit maxima at 6 or 7 GPa and then decrease at higher pressures. The sizes of z-BN crystals grown from Si_3N_4-bearing t-BN show little change with temperature after their appearance at 1500 or 1600° C.

Composite compacts are obtained through spontaneous sintering at high pressure–high temperature. Some mechanical properties are measured specifically for the compacts obtained from t-BN/β-Si_3N_4 (10.6 wt %): Vickers microhardness as high as 60 GPa. Young's modulus of 570 GPa, and fracture toughness higher than 5.5 MPa $m^{1/2}$.

Acknowledgements

This work was supported in part by the Development Corporation of Japan under the programme for ERATO. We thank Professor T. Masumoto for supervision, Dr J. Umemura and Ms E. Okamura for help with the infrared measurements and Mr T. Ashida for the SEM observation.

References

1. "Frontiers in Materials Technologies", edited by M. A. Meyers and O. T. Inal (Elsevier, Amsterdam, 1985).
2. A. ONODERA, N. TAKAHASHI, H. YOSHIHARA, H. NAKAE, Y. MATSUNAMI and T. HIRAI, *J. Mater. Sci.* **25** (1990) in press.
3. R. H. WENTORF Jr., R. C. DeVRIES and F. P. BUNDY, *Science* **208** (1980) 873.
4. J. THOMAS Jr, N. E. WESTON and T. E. O'CONNER, *J. Amer. Chem. Soc.* **84** (1963) 4619.
5. T. MATSUDA, H. NAKAE and T. HIRAI, *J. Mater. Sci.* **21** (1986) 649.
6. H. NAKAE, Y. MATSUNAMI, N. UNO, T. MATSUDA and T. HIRAI, in "Proceedings of the 5th European Conference on Chemical Vapour Deposition", edited by J.-O. Carlsson and J. Lindström, (Uppsala University, Uppsala, 1985) p. 242.
7. M. J. RAND and J. F. ROBERTS, *J. Electrochem. Soc.* **115** (1968) 428.
8. N. WADA, S. A. SOLIN, J. WONG and S. PROCHAZKA, *J. Noncryst. Solids* **43** (1981) 7.
9. H. NAKAE, Y. MATSUNAMI and T. HIRAI, unpublished.
10. N. KAWAI, M. TOGAYA and A. ONODERA, *Proc. Jpn. Acad.* **47** (1974) 623.
11. A. ONODERA, *High Temp. High Press.* **19** (1987) 579.
12. A. OHTANI, S. MIZUKAMI, M. KATAYAMA, A. ONODERA and N. KAWAI, *Jpn. J. Appl. Phys.* **16** (1977) 1843.
13. A. ONODERA and A. OHTANI, *J. Appl. Phys.* **51** (1980) 2581.
14. S. SASAKURA, K. SUITO and H. FUJISAWA, in "High Pressure Science and Technology", Vol. 2, edited by N. V. Novikov (Naukova Dumka, Kiev, 1989) p. 60.
15. K. NIIHARA, R. MORENA and D. P. H. HASSELMAN, *J. Mater. Sci. Lett.* **1** (1982) 13.
16. I. S. GLADKAYA, G. N. KREMKOVA and V. N. SLESAREV, *J. Less-Common Metals* **117** (1986) 241.
17. N. N. SIROTA and N. A. KOFMAN, *Sov. Phys. Doklady* **24** (1979) 1001.
18. H. SUMIYA, T. ISEKI and A. ONODERA, *Mater. Res. Bull.* **18** (1983) 1203.
19. K. ICHINOSE, M. WAKASUKI, T. AOKI and Y. MAEDA, in "Proceedings of the 4th International Conference on High Pressure", edited by J. Osugi (Physicochemical Society of Japan, Kyoto, 1974) p. 436.
20. A. ONODERA, H. SUMIYA, N. TAKAHASHI, K. HIGASHI, R. OHSHIMA, H. SAKA, K. NOBUGAI and F. KANAMARU, in preparation.
21. B. D. CULLITY, "Elements of X-ray Diffraction" (Addison-Wesley, Reading, 1956).
22. R. C. DeVRIES, "Cubic Boron Nitride: Handbook of Properties", GE Technical Report 72CRD178 (1972).
23. S. HIRANO, S. HON and S. NAKA, in "High Pressure Science and Industry", edited by C.-M. Backman, T. Johannisson and L. Tegnér (Arkitektkopia, Uppsala, 1982) p. 376.
24. E. RAPOPORT, K. SATO and S. SAWAOKA, *ibid.*, p. 384.
25. B. K. AGARWALA, B. P. SINGH and S. K. SINGHAL, *J. Mater. Sci.* **7** (1986) 1765.
26. M. WAKATSUKI, K. ICHINOSE and T. AOKI, *Mater. Res. Bull.* **7** (1972) 999.
27. A. SAWAOKA, S. SAITO and M. ARAKI, in "High Pressure Science and Technology", Vol. 1, edited by K. D. Timmerhaus and M. S. Barber (Plenum, New York, 1979) p. 986.
28. S. SAITO and A. SAWAOKA, in "High Pressure Science and Technology", Vol. 2, edited by B. Vodar and Ph. Marteau (Pergamon, London, 1981) p. 541.
29. S. PROCHAZKA and W. A. ROCCO, *High Temp. High Press.* **10** (1978) 87.
30. W. POMPE, H. A. BARI, G. GILLE, W. KREHER, B. SCULTRICH and H.-J. WEISS, in "Current Topics in Material Science", Vol. 12, edited by E. Kaldis (Elsevier, Amsterdam, 1985) Ch. 4.
31. J. T. NEIL, *Mater. Engng* March (1984) 36.
32. V. I. MATKOVICH, *Acta Crystallogr.* **13** (1960) 679.
33. D. HARDE and K. H. JACK, *Nature* **160** (1957) 332.
34. M. SHIMADA, N. OGAWA, M. KOIZUMI, F. DACHILLE and R. ROY, *Amer. Ceram. Soc. Bull.* **58** (1979) 519.
35. T. YAMADA, T. TANAKA, M. SHIMADA and M. KOIZUMI, *J. Mater. Sci. Lett.* **1** (1982) 455.
36. F. P. BUNDY and R. H. WENTORF Jr, *J. Chem. Phys.* **38** (1963) 1144.

37. M. WAKATSUKI and K. ICHINOSE, in "Proceedings of the 4th International Conference on High Pressure", edited by J. Osugi (Physicochemical Society of Japan, Kyoto, 1974) p. 441.
38. I. N. FRANTSEVICH, T. R. BALAN, A. V. BOCHKO, S. S. DZHMAROV, G. G. KARYUK, A. V. KURDYUMOV and A. U. PILYANKEVICH, *Dokl. Akad. Nauk SSSR* **218** (1974) 591.
39. A. ONODERA, K. INOUE, H. YOSHIHARA, H. NAKAE, T. MATSUDA and T. HIRAI, *J. Mater. Sci.* **25** (1990) in press.
40. F. R. CORRIGAN and F. P. BUNDY, *J. Chem. Phys.* **63** (1975) 3812.

Received 31 May
and accepted 23 October 1989